Biointerface Research in Applied Chemistry
Open-Access Journal (ISSN: 2069-5837)

Article
Volume 13, Issue 5, 2023, 497
https://doi.org/10.33263/BRIAC135.497

Insights into the Delivery of Hydrea Anticancer Drug by the Assistance of an Oxidized Silicon Carbide Nanocage

Muhammad Da'i [1,*], Arifah Sri Wahyuni [1], Erindyah Retno Wikantyasning [1], Maryati [1], Mahmoud Mirzaei [2,*]

[1] Faculty of Pharmacy, Universitas Muhammadiyah Surakarta, Surakarta, Indonesia; muhammad.dai@ums.ac.id (M.D.); arifah.wahyuni@ums.ac.id (A.S.W.); erindyah.rw@ums.ac.id (E.R.W.); maryati@ums.ac.id (M.);
[2] Child Growth and Development Research Center, Research Institute for Primordial Prevention of Non-Communicable Disease, Isfahan University of Medical Sciences, Isfahan, Iran; mirzaei.res@gmail.com (M.M.);
* Correspondence: mdai.muhammad.dai@ums.ac.id (M.D.); mirzaei.res@gmail.com (M.M.);
Scopus Author ID 57189357187 (M.D.)
13204227300 (M.M.)
Received: 25.09.2022; Accepted: 30.10.2022; Published: 6.01.2023

Abstract: Hydrea (HYD) or hydroxyurea is a known anticancer, in which its combination with a representative model of oxidized silicon carbide (OSiC) nanocage was investigated in this work to provide insights into the drug delivery approach. To this aim, density functional theory (DFT) calculations were performed to optimize the models and evaluate their features. Exploring different configurations of interactions between HYD and OSiC yielded four HYD@OSiC bimolecular complexes regarding the involvement of different molecular sites of substances in interactions. Interactions between each of the H1 to H4 bimolecular complexes were found to be at a reasonable level of energy strength assigned by adsorption energy. Accordingly, the OSiC substance was found as an adsorbent of the HYD substance with a significant role in managing the whole system based on the obtained molecular orbital features. Details of interactions were determined by performing additional quantum theory of atoms in molecules (QTAIM) on the optimized bimolecular models showing the existence of two interactions with meaningful strengths in each of the H1 to H4 models. Based on all the obtained results, the models of HYD@OSiC were found suitable to be proposed for employment in drug delivery applications. Indeed, the current research indicated the benefits of employing the OSiC substance for an oriented delivery of the HYD anticancer drug substance.

Keywords: Hydrea; silicon carbide; nanocage; anticancer; drug delivery; DFT.

1. Introduction

Nanostructures have been found as useful materials for employment in various types of applications, from industries up to living systems, since their innovation in 1991 [1-5]. Different structural forms of nanostructures, including tubular, planar, and spherical, besides some other forms, have been obtained to this time [6-10]. Among the expected applications of nanostructures, employing them in drug delivery-related processes were of the highest importance due to the development of more efficient therapeutic tools for treating health systems [11]. Accordingly, earlier studies investigated the benefits of nanostructures for employment in drug delivery platforms [12-15]. Indeed, the high surface area of nanostructures is an advantage for participating in adsorption processes towards other substances [16-18]. The pure carbon nanostructures and combined atomic compositions could work for approaching

adsorption purposes [19-22]. Several attempts have been made to learn the real benefits of nanostructures for employment in drug delivery-related platforms, but the achievements are not yet certain [23-25]. The drug delivery purposes and several biomedical applications were explored for the nanostructures [26-30]. To this point, further investigations are still required, in which the current work was done to reveal insights into the delivery of Hydrea anticancer drug with the assistance of an oxidized silicon carbide nanocage.

Anticancer agents are among those critical drugs with advantages/disadvantages for medicating cancer patients, and their improvements are always required [31-35]. Hydrea, or hydroxyurea, is a known anticancer drug for treating different cancers [36]. Considerable efforts have been dedicated to improving the efficiency of hydra for conducting a more efficient treatment of cancer patients up to now [37-40]. By the expected functions of nanostructures for working in the drug delivery platforms, examining details of complexes of nanostructures and Hydrea could help to provide more insights into developing such a hypothesis of nano-assisted delivery of this drug. To this aim, interactions between the Hydrea anticancer drug and a model of oxidized silicon carbide nanocage were investigated within the current work. The investigated models were stabilized, and their features were evaluated to discuss the major goal of this work for providing insights into the delivery of hydra anticancer with the assistance of an oxidized silicon carbide nanocage. It is worth mentioning that the existence of silicon carbide nanostructures was identified by earlier works [41-43]. The 3D structures of singular and bimolecular models were optimized to provide the required information for discussing the related issues by benefits of performing density functional theory (DFT) calculations in such cases [44-48]. The investigated singular and bimolecular models were exhibited in Figures 1 and 2, and their evaluated quantitative features were tabulated in Tables 1 and 2.

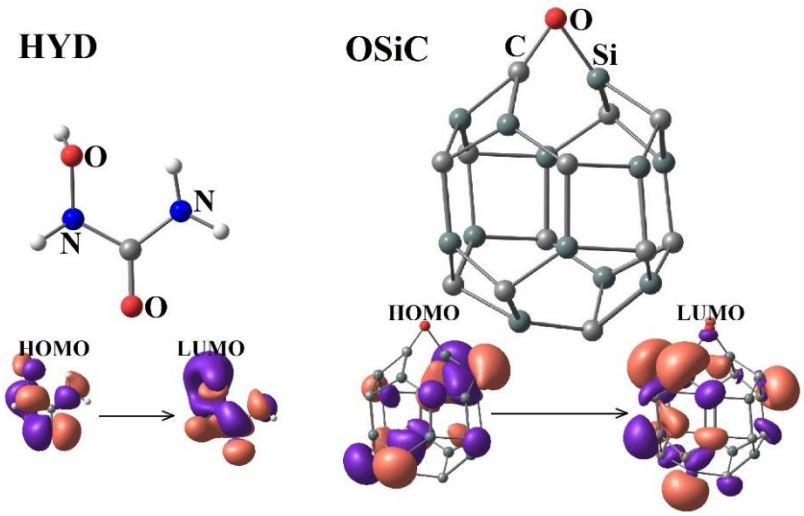

Figure 1. The singular models of Hydrea (HYD) and oxidized silicon carbide (OSiC) nanocage and their frontier molecular orbitals (HOMO and LUMO) representations.

2. Materials and Methods

The parental models of this work (Figure 1) were the Hydrea (HYD) anticancer and the oxidized silicon carbide (OSiC) nanocage, in which they were optimized to find their stabilized geometries in correspondence with the minimized energy level. Subsequently, the already optimized singular models were combined to create the HYD@OSiC bimolecular models (Figure 2). Finally, by examining all possibilities of configurational variations of two

molecules towards each other, four optimized bimolecular models, H1-H4, were obtained by performing re-optimization calculations.

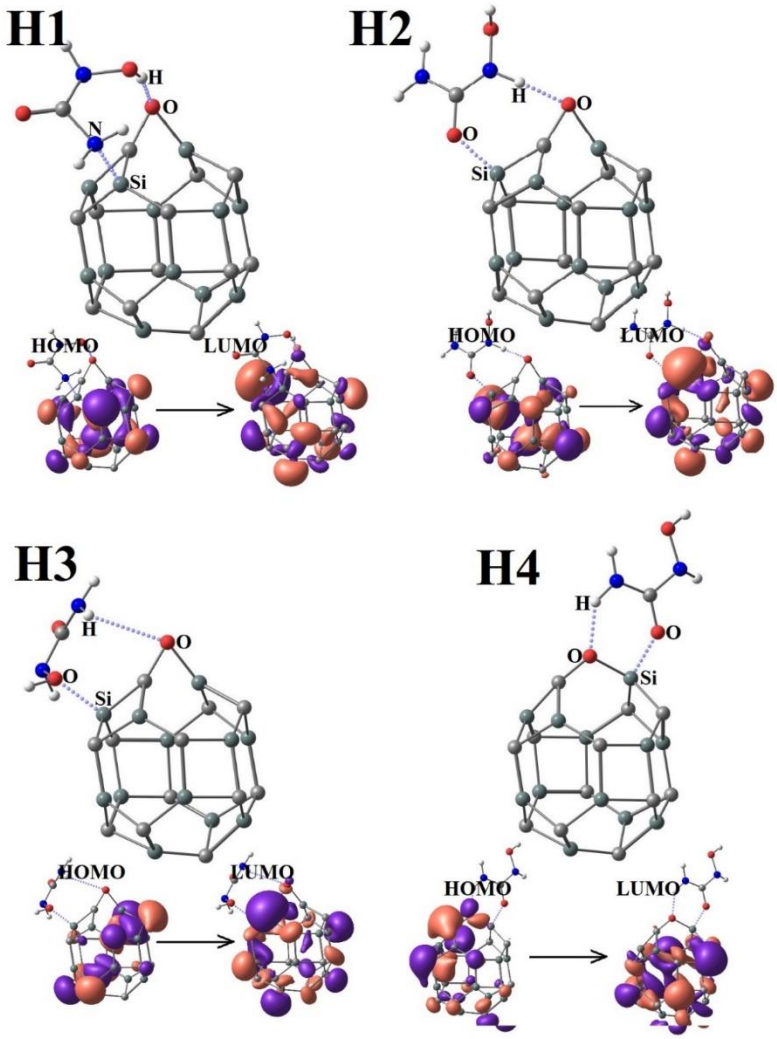

Figure 2. The bimolecular models of HYD@OSiC complexes, H1-H4, and their frontier molecular orbitals (HOMO and LUMO) representations.

As listed in Table 1, molecular features of singular and bimolecular models were evaluated to describe the investigated model systems. The highest occupied molecular orbital (HOMO) and the lowest unoccupied molecular orbital (LUMO) are both very important for assigning electronic communications of molecular models, which were obtained in this work in both quantitative and quantitative energies of E_{HOMO} and E_{LUMO} and graphical representations of distribution patterns. Additionally, values of energy gap (E_{Gap}) and chemical hardness (C_{Hard}) were obtained as $E_{Gap} = E_{LUMO} - E_{HOMO}$, and $C_{Hard} = E_{Gap}/2$. Accordingly, the models were analyzed based on their molecular electronics features. E_{Ads} implied for the energy of adsorption of HYD at the OSiC surface indicated by energy differences of bimolecular and singular states as $E_{Ads} = E_{HYD@OSiC} - E_{HYD} - E_{OSiC}$. The impacts of basis set superposition error (BSSE) [49] on the evaluated values of E_{Ads} were almost negligible. In Table 2, further details of interactions of bimolecular models were provided by the evaluated features of quantum theory of atoms in molecules (QTAIM) analyses [50]. Interactions types and distances, and values of total electron density ($\nabla^2\rho$), Laplacian of electron density (ρ), and energy density (H), were evaluated to recognize details of interacting systems. The B3LYP-D3/6-31G* DFT calculations were performed to obtain the optimized structures and their related features using the Gaussian program [51, 52]. Other software, including GaussView, ChemCraft, and

MultiWfn, were employed for extracting the results [53-55]. Consequently, the models were prepared, and their features were evaluated to provide insights into the delivery of HYD anticancer drugs with the assistance of an OSiC cage.

3. Results and Discussion

Providing insights into the delivery of Hydrea (HYD) anticancer drug with the assistance of oxidized silicon carbide (OSiC) nanocage was done in this work by means of performing DFT calculations. The parental models were exhibited in Figure 1, including the singular models of HYD and OSiC. To create an oxidized form of SiC nanocage, an additional oxygen atom was added to the structures to make a representative model of oxidized SiC nanocage assigned by OSiC. The models were optimized, and their stabilized geometries were found to involve them in interactions for creating HYD@OSiC models (Figure 2). All possibilities of HYD and OSiC substances' relaxation possibilities were examined, and four models were obtained, including H1, H2, H3, and H4. In each model, the occurred interactions between HYD and OSiC conducted the formation of bimolecular complexes. Different configurations were also obtained based on involving different modular sites of models in interactions. To figure out the electronic properties, the molecular features of the investigated models are listed in Table 1.

Table 1. Molecular features of singular and bimolecular models.[1]

Model	Formula	E_{HOMO} (eV)	E_{LUMO} (eV)	E_{Gap} (eV)	C_{Hard} (eV)	E_{Ads} (eV)
HYD	$CH_4N_2O_2$	-6.964	0.962	7.925	3.963	–
OSiC	$C_{12}OSi_{12}$	-6.039	-2.991	3.047	1.524	–
H1	$C_{13}H_4N_2O_3Si_{12}$	-5.682	-2.560	3.123	1.561	-1.334
H2	$C_{13}H_4N_2O_3Si_{12}$	-5.291	-2.234	3.057	1.529	-1.720
H3	$C_{13}H_4N_2O_3Si_{12}$	-5.820	-2.695	3.126	1.563	-0.884
H4	$C_{13}H_4N_2O_3Si_{12}$	-4.862	-1.944	2.917	1.459	-1.457

[1]The models were shown in Figures 1 and 2.

As found by the energy values of HOMO and LUMO, the models were in different levels of contributions to electron transfer processes. HOMO is indeed a level of electron-donating, and LUMO is a level of electron-accepting, in which different levels of molecules could help to reach a point of electron transferring process. A careful examination of HOMO and LUMO levels of HYD and OSiC could reveal the direction of electron transfer from HYD to OSiC as the HOMO level of HYD was lower than that of OSiC, and the LUMO of HYD was upper than that of OSiC. Accordingly, electron transferring could be taken place from HOMO of HYD to HOMO of OSiC and from LUMO of HYD to LUMO of OSiC. This claim could be very well affirmed by the exhibited distribution patterns of Figure 2, in which both HOMO and LUMO were moved to the OSiC substance of all of the H1, H2, H3, and H4 bimolecular complexes. This achievement could be a clue of the benefit of employing the OSiC substance for efficiently adsorbing the HYD substance for approaching drug delivery purposes. As could be found by the HOMO and LUMO results, the OSiC adsorbent could manage further contributions of the adsorbed HYD substance to other interactions.

In addition to the exact energy values of HOMO and LUMO, differences between the two levels are also very important for recognizing the electronic features of molecular systems. As found for the models, the values of energy gaps (E_{Gap}) of bimolecular models were closer to the value of singular OSiC, showing this adsorbent's significant impact on adsorbent HYD substance. This achievement agrees with the earlier achievement of movement of both HOMO and LUMO patterns to the OSiC substance. Accordingly, the values of E_{Gap} affirmed such

observation for the molecular orbitals features. In other words, the significant role of OSiC was affirmed for conducting the further behaviors of adsorbed HYD substance for approaching a targeted delivery process. Smaller values of chemical hardness (C_{Hard}) also affirmed the benefits of bimolecular complexes for contributing to more efficient reactions or interactions compared with the singular HYD substance. The values of adsorption energy (E_{Ads}) also approved formations of HYD@OSiC bimolecular complexes by assigning reasonable strength values for the model systems. Compared to the results of earlier parallel works [40, 56-58], the current models were found suitable for achieving strong complexes. Based on the obtained results, H2 was found at the highest level of strength, and H3 was found at the lowest level in the order of H2 > H4 > H1 > H3. It is noted that examining all possibilities of interactions was important to learn details of interactions strength, in which different meaningful adsorption strengths and configurations were found for the HYD@OSiC bimolecular models. To this point, further details of such interactions were evaluated by performing QTAIM analyses on the optimized bimolecular models.

Table 2. Interactions features of bimolecular models.[1]

HYD@OSiC	Interaction	Distance (Å)	ρ (au)	$\nabla^2\rho$ (au)	H (au)
H1	H…O N…Si	1.713 1.998	0.044 0.071	0.139 0.294	-0.002 -0.018
H2	H…O O…Si	1.732 1.813	0.042 0.083	0.137 0.437	-0.001 -0.027
H3	H…O O…Si	2.798 1.953	0.004 0.063	0.019 0.216	0.001 -0.016
H4	H…O O…Si	1.811 1.816	0.036 0.082	0.121 0.416	-0.001 -0.026

[1]The models were shown in Figure 2.

Details of QTAIM analyses for the interactions of HYD@OSiC bimolecular models are listed in Table 2. As shown in Figure 2, two interactions were involved in each bimolecular model assigned by the types of interactions in Table 2. Within the models, H…O interactions were available for all four bimolecular models. Next, N…Si was available for H1, and O…Si was available for H2-H4. Accordingly, different values of distances and interaction descriptions were found for the models. Careful examinations of the results could indicate the significant roles of relaxations configurations for achieving string adsorption, in which H2 was at the highest level of strength among H1-H4 models. H…O and O…Si were two interactions of this model with significant levels of QTAIM descriptions. Accordingly, the model was found to be at the highest strength level of adsorption. In all other cases, the levels of strengths and the obtained results helped to learn details of interactions between HYD and OSiC substances with different levels of strengths. Indeed, based on such QTAIM features, the models were recognized by their details of interactions to learn their structural configurations for creating bimolecular models. Not only the type of interactions but the roles of all interactions were found in this case. Learning the basics of creating such configuration could help make an oriented application for the models' systems as found for the HYD@OSiC complexes for assigning their further applications of drug delivery processes.

4. Conclusions

The majority of this work was to provide insights into the delivery of HYD anticancer drugs with the assistance of an OSiC nanocage. To this aim, DFT calculations were performed to optimize the structures and to evaluate their related features. The results indicated the

existence of four different configurations of HYD@OSiC bimolecular complexes with meaningful levels of adsorption strengths. Additionally, the molecular orbital features indicated a significant role of OSiC substance in managing the adsorption process and the adsorbed HYD substance's behaviors for further reactions and interactions. Movements of HOMO and LUMO patterns to the OSiC substance and a closer value of E_{Gap} of bimolecular models to that of the single OSiC substance than the single HYD substance all approved the significant role of OSiC. Additionally, analyzing details of interactions indicated the existence of types of specific interactions and their descriptions. To conclude the obtained results of this work, it could be mentioned that the models of HYD@OSiC were found suitable to be proposed for the drug delivery process.

Funding

This research received no external funding.

Acknowledgments

This research has no acknowledgment.

Conflicts of Interest

The authors declare no conflict of interest.

References

1. Talebian, S.; Rodrigues, T.; Das Neves, J.; Sarmento, B.; Langer, R.; Conde, J. Facts and figures on materials science and nanotechnology progress and investment. *ACS Nano* **2021,** *15,* 15940, https://doi.org/10.1021/acsnano.1c03992.
2. Ahmed, M.; Dekhyl, A.; Alwan, L. Preparation and characterization of nano-carbon as an adsorbent for industrial water treatment. *Eurasian Chemical Communications* **2022,** *4,* 852, https://doi.org/10.22034/ecc.2022.332809.1356.
3. Saliminasab, M.; Jabbari, H.; Farahmand, H.; Asadi, M.; Soleimani, M.; Fathi, A. Study of antibacterial performance of synthesized silver nanoparticles on Streptococcus mutans bacteria. *Nanomedicine Research Journal* **2022,** *7,* 391, https://doi.org/10.22034/nmrj.2022.04.010.
4. Shete, R.; Fernandes, P.; Borhade, B.; Pawar, A.; Sonawane, M.; Warude, N. Review of cobalt oxide nanoparticles: green synthesis, miomedical applications, and toxicity studies. *Journal of Chemical Reviews* **2022,** *4*,331, https://doi.org/10.22034/jcr.2022.342398.1172.
5. Dessie, Y.; Tadesse, S. A review on advancements of nanocomposites as efficient anode modifier catalyst for microbial fuel cell performance improvement. *Journal of Chemical Reviews* **2021,** *3,* 320, https://doi.org/10.22034/jcr.2021.314327.1128.
6. Wu, Y.; Zhao, X.; Shang, Y.; Chang, S.; Dai, L.; Cao, A. Application-driven carbon nanotube functional materials. *ACS Nano* **2021,** *15,* 7946, https://doi.org/10.1021/acsnano.0c10662.
7. Wang, M.; Huang, M.; Luo, D.; Li, Y.; Choe, M.; Seong, W.K.; et al. Single-crystal, large-area, fold-free monolayer graphene. *Nature* **2021,** *596,* 519, https://doi.org/10.1038/s41586-021-03753-3.
8. Hou, L.; Cui, X.; Guan, B.; Wang, S.; Li, R.; Liu, Y.; et al. Synthesis of a monolayer fullerene network. *Nature* **2022,** *606,* 507, https://doi.org/10.1038/s41586-022-04771-5.
9. Zilabi, S.; Shareei, M.; Bozorgian, A.; Ahmadpour, A.; Esmaeil, E. A review on nanoparticle application as an additive in lubricants. *Advanced Journal of Chemistry-Section B* **2022,** *4,* 209, https://doi.org/10.22034/ajcb.2022.353097.1125.
10. Sinha, N.J.; Langenstein, M.G.; Pochan, D.J.; Kloxin, C.J.; Saven, J.G. Peptide design and self-assembly into targeted nanostructure and functional materials. *Chemical Reviews* **2021,** *121,* 13915, https://doi.org/10.1021/acs.chemrev.1c00712.

11. Hatami, A.; Heydarinasab, A.; Akbarzadehkhiyavi, A.; Pajoum Shariati, F. An introduction to nanotechnology and drug delivery. *Chemical Methodologies* **2021,** *5*, 153, https://doi.org/10.22034/chemm.2021.121496.
12. Wang, J.; Li, Y.; Nie, G. Multifunctional biomolecule nanostructures for cancer therapy. *Nature Reviews Materials* **2021,** *6*, 766, https://doi.org/10.1038/s41578-021-00315-x.
13. Sukmawati, A.; Da'i, M.; Yuliani, R.; Anggraeni, S.N.; Wahyuningsih, D. Characterization of chitosan nanoparticle containing combination doxorubicin and curcumin analogue. *Advanced Science Letters* **2017,** *23*, 12486, https://doi.org/10.1166/asl.2017.10798.
14. Ali Fadhil, H.; H. Samir, A.; Abdulghafoor Mohammed, Y.; Al Rubaei, ZM.M. Synthesis, characterization, and in vitro study of novel modified reduced graphene oxide (RGO) containing heterocyclic compounds as anti-breast cancer. *Eurasian Chemical Communications* **2022,** *4*, 1156, https://doi.org/10.22034/ecc.2022.345188.1484.
15. Sukmawati, A.; Utami, W.; Yuliani, R.; Da'i, M.; Nafarin, A. Effect of tween 80 on nanoparticle preparation of modified chitosan for targeted delivery of combination doxorubicin and curcumin analogue. *IOP Conference Series: Materials Science and Engineering* **2018,** *311*, 012024, https://doi.org/10.1088/1757-899X/311/1/012024.
16. Ghiasi, R.; Valizadeh, A. Interaction of cisplatin anticancer drug with C 20 bowl: DFT investigation. *Main Group Chemistry* **2022,** *21*, 43, https://doi.org/10.3233/MGC-210076.
17. Dhumad, A.M.; Majeed, H.J.; Zandi, H.; Harismah, K. FeC19 cage vehicle for fluorouracil anticancer drug delivery: DFT approach. *Journal of Molecular Liquids* **2021,** *333*, 115905, https://doi.org/10.1016/j.molliq.2021.115905.
18. Harismah, K.; Shahrtash, S.A., Arabi, A.R.; Khadivi, R.; Mirzaei, M.; Akhavan-Sigari, R. Favipiravir attachment to a conical nanocarbon: DFT assessments of the drug delivery approach. *Computational and Theoretical Chemistry* **2022,** *1216*, 113866, https://doi.org/10.1016/j.comptc.2022.113866.
19. Farhami, N. A computational study of thiophene adsorption on boron nitride nanotube. *Journal of Applied Organometallic Chemistry* **2022,** *2*, 163, https://doi.org/10.22034/jaoc.2022.154821.
20. Darougari, H.; Rezaei-Sameti, M. The drug delivery appraisal of Cu and Ni decorated B12N12 nanocage for an 8-hydroxyquinoline drug: a DFT and TD-DFT computational study. *Asian Journal of Nanosciences and Materials* **2022,** *5*, 196, http://www.ajnanomat.com/article_154625.html.
21. Golipour-Chobar, E.; Salimi, F.; Ebrahimzadeh-Rajaei, G. Sensing of lomustine drug by pure and doped C48 nanoclusters: DFT calculations. *Chemical Methodologies* **2022,** *6*, 790, https://doi.org/10.22034/chemm.2022.344895.1555.
22. Anafcheh, M. A comparison between density functional theory calculations and the additive schemes of polarizabilities of the Li-F-decorated BN cages. *Journal of Applied Organometallic Chemistry* **2021,** *1*, 125, https://doi.org/10.22034/jaoc.2021.292384.1027.
23. Sahu, T.; Ratre, Y.K.; Chauhan, S.; Bhaskar, L.V.; Nair, M.P.; Verma, H.K. Nanotechnology based drug delivery system: current strategies and emerging therapeutic potential for medical science. *Journal of Drug Delivery Science and Technology* **2021,** *63*, 102487, https://doi.org/10.1016/j.jddst.2021.102487.
24. Mortezagholi, B.; Movahed, E.; Fathi, A.; Soleimani, M.; Forutan Mirhosseini, A.; Zeini, N.; Khatami, M.; Naderifar, M.; Abedi Kiasari, B.; Zareanshahraki, M. Plant-mediated synthesis of silver-doped zinc oxide nanoparticles and evaluation of their antimicrobial activity against bacteria cause tooth decay. *Microscopy Research and Technique* **2022,** *85*, 3553, https://doi.org/10.1002/jemt.24207.
25. Mohajer, F.; Mohammadi Ziarani, G.; Badiei, A. New advances on Modulating nanomagnetic cores as the MRI-monitored drug release in cancer. *Journal of Applied Organometallic Chemistry* **2021,** *1*, 143, https://doi.org/10.22034/jaoc.2021.301405.1032.
26. Molani, F.; Veisi, F.; Mohammadiazar, S. A nano-bio-eco interaction to synthesis of gold nanoparticles using tribulus terrestris extract and its antibacterial activity. *Advanced Journal of Chemistry-Section A*, **2021,** *4*, 197, https://doi.org/10.22034/ajca.2021.262453.1231.
27. Hatami, A. Preparation, description and evaluation of the lethality acid loaded liposomal nanoparticles against in vitro colon and liver cancer. *Journal of Chemical Reviews* **2021,** *3*, 121, https://doi.org/10.22034/jcr.2021.283609.1109.
28. Tosan, F.; Rahnama, N.; Sakhaei, D.; Fathi, A.; Yari, A. Effects of doping metal nanoparticles in hydroxyapatite in Improving the physical and chemical properties of dental implants. *Nanomedicine Research Journal* **2021,** *6*, 327, https://doi.org/10.22034/nmrj.2021.04.002.

29. Alizadeh, S.; Nazari, Z. Amphetamine, methamphetamine, morphine @ AuNPs kit based on PARAFAC. *Advanced Journal of Chemistry-Section A* **2022,** *5*, 253, https://doi.org/10.22034/ajca.2022.345350.1318.
30. Aminian, A.; Fathi, A.; Gerami, M.H.; Arsan, M.; Forutan Mirhosseini, A.; Torabizadeh, S.A. Nanoparticles to overcome bacterial resistance in orthopedic and dental implants. *Nanomedicine Research Journal* **2022,** *7*, 107, https://doi.org/10.22034/nmrj.2022.02.001.
31. Nussinov, R.; Tsai, C.J.; Jang, H. Anticancer drug resistance: an update and perspective. *Drug Resistance Updates* **2021,** *59*, 100796, https://doi.org/10.1016/j.drup.2021.100796.
32. Garcia-Oliveira, P.; Otero, P.; Pereira, A.G.; Chamorro, F.; Carpena, M.; Echave, J.; Fraga-Corral, M.; Simal-Gandara, J.; Prieto, M.A. Status and challenges of plant-anticancer compounds in cancer treatment. *Pharmaceuticals* **2021,** *14*, 157, https://doi.org/10.3390/ph14020157.
33. Hatami, A.; Azizi Haghighat, Z. Evaluation of application of drug modeling in treatment of liver and intestinal cancer. *Progress in Chemical and Biochemical Research* **2021,** *4*, 220, https://doi.org/10.22034/pcbr.2021.277514.1181.
34. Hudiyawati, D.; Syafitry, W. Effectiveness of physical and psychological treatment for cancer-related fatigue: systematic review. *Jurnal Kesehatan* **2021,** *14*, 195, https://doi.org/10.23917/jk.v14i2.15596.
35. Saroyo, H.; Saputri, N.F. Cytotoxicity of mangrove leaves (rhizophora) ethanolic extract on cancer cells. *Journal of Nutraceuticals and Herbal Medicine* **2021,** *4*, 43, https://doi.org/10.23917/jnhm.v4i1.15657.
36. Musiałek, M.W.; Rybaczek, D. Hydroxyurea-the good, the bad and the ugly. *Genes* **2021,** *12*, 1096, https://doi.org/10.3390/genes12071096.
37. Alharbi, W. Advancement and recent trends in seeking less toxic and more active anticancer drugs: Insights into thiourea based molecules. *Main Group Chemistry* **2022,** *21*, 885, https://doi.org/10.3233/MGC-210183.
38. Ansari, S.H.; Ansari, I.; Wasim, M.; Sattar, A.; Khawaja, S.; Zohaib, M.; et al. Evaluation of the combination therapy of hydroxyurea and thalidomide in β-thalassemia. *Blood Advances* **2022,** *in press*, https://doi.org/10.1182/bloodadvances.2022007031.
39. Rahimi, R.; Solimannejad, M.; Ehsanfar, Z. Potential application of XC3 (X= B, N) nanosheets in drug delivery of hydroxyurea anticancer drug: a comparative DFT study. *Molecular Physics* **2022,** *120*, e2014587, https://doi.org/10.1080/00268976.2021.2014587.
40. Kadhim, M.M.; Sheibanian, N.; Ashoori, D.; Sadri, M.; Tavakoli-Far, B.; Khadivi, R.; Akhavan-Sigari, R. The drug delivery of hydrea anticancer by a nanocone-oxide: computational assessments. *Computational and Theoretical Chemistry* **2022,** *1215*, 113843, https://doi.org/10.1016/j.comptc.2022.113843.
41. Li, J.; Xia, Y.; Zhao, M.; Liu, X.; Song, C.; Li, L.; et al. From a fullerene-like cage (SiC)12 to novel silicon carbide nanowires: an ab initio study. *Chemical Physics Letters* **2007,** *442*, 384, https://doi.org/10.1016/j.cplett.2007.06.008.
42. Wang, C.H.; Chang, Y.H.; Yen, M.Y.; Peng, C.W.; Lee, C.Y.; Chiu, H.T. Synthesis of silicon carbide nanostructures via a simplified Yajima process- reaction at the vapor - liquid interface. *Advanced Materials* **2005,** *17*, 419, https://doi.org/10.1002/adma.200400939.
43. Huda, M.N.; Ray, A.K. Novel silicon-carbon fullerene-like cages. *The European Physical Journal D-Atomic, Molecular, Optical and Plasma Physics* **2004,** *31*, 63, https://doi.org/10.1140/epjd/e2004-00128-9.
44. Wang, W.; Ye, Z.; Gao, H.; Ouyang, D. Computational pharmaceutics- a new paradigm of drug delivery. *Journal of Controlled Release* **2021,** *338*, 119, https://doi.org/10.1016/j.jconrel.2021.08.030.
45. Mohamed, H.; Hamza, Z.; Nagdy, A.; El-Mageed, H. Computational studies and DFT calculations of synthesized triazolo pyrimidine derivatives: a review. *Journal of Chemical Reviews* **2022,** *4*, 156, https://doi.org/10.22034/jcr.2022.325439.1138.
46. Ghiasifar, M.; hosseinnejad, T.; Ahangar, A. Copper catalyzed cycloaddition reaction of azidomethyl benzene with 2,2-di(prop-2-yn-1-yl)propane-1,3-diol: DFT and QTAIM investigation. *Progress in Chemical and Biochemical Research* **2022,** *5*, 1, https://doi.org/10.22034/pcbr.2022.319090.1203.
47. Esan, T.; Oyeneyin, O.; Olanipekun, A.; Ipinloju, N. Corrosion inhibitive potentials of some amino acid derivatives of 1,4-naphthoquinone–DFT calculations. *Advanced Journal of Chemistry-Section A* **2022,** *5*, 263, https://doi.org/10.22034/ajca.2022.353882.1321.
48. Akinlosotu, O.; Ogunyemi, B.; Adeleke, B. Substituent effect on bithiophene-bipyridine organic conjugated systems: theoretical investigation. *Advanced Journal of Chemistry-Section A* **2022,** *5*, 70, https://doi.org/10.22034/ajca.2022.320173.1290.
49. Davidson, E.R.; Chakravorty, S.J. A possible definition of basis set superposition error. *Chemical Physics Letters* **1994,** *217*, 48, https://doi.org/10.1016/0009-2614(93)E1356-L.

50. Bader, R.F.; Matta, C.F. Atomic charges are measurable quantum expectation values: a rebuttal of criticisms of QTAIM charges. *The Journal of Physical Chemistry A* **2004,** *108*, 8385, https://doi.org/10.1021/jp0482666.
51. Moellmann, J.; Grimme, S. DFT-D3 study of some molecular crystals. *The Journal of Physical Chemistry C* **2014,** *118*, 7615, https://doi.org/10.1021/jp501237c.
52. Frisch, M.J.; Trucks, G.W.; Schlegel, H.B.; Scuseria, G.E.; Robb, M.A.; Cheeseman, J.R.; et al. Gaussian 09 program. *Gaussian Inc.* Wallingford, CT, **2009.**
53. Dennington, R.; Keith, T.A.; Millam, J.M. GaussView. *Semichem Inc.*, Shawnee Mission, KS, **2016.**
54. Chemcraft. https://www.chemcraftprog.com.
55. Lu, T.; Chen, F. Multiwfn: a multifunctional wavefunction analyzer. *Journal of Computational Chemistry* **2012,** *33*, 580, https://doi.org/10.1002/Jcc.22885.
56. Li, W.; Zhao, T. Hydroxyurea anticancer drug adsorption on the pristine and doped C70 fullerene as potential carriers for drug delivery. *Journal of Molecular Liquids* **2021,** *340*, 117226, https://doi.org/10.1016/j.molliq.2021.117226.
57. Mirzaei, M.; Gulseren, O.; Rafienia, M.; Zare, A. Nanocarbon-assisted biosensor for diagnosis of exhaled biomarkers of lung cancer: DFT approach. *Eurasian Chemical Communications* **2021,** *3*, 154, https://doi.org/10.22034/ecc.2021.269256.1126.
58. Kouchaki, A.; Gülseren, O.; Hadipour, N.; Mirzaei, M. Relaxations of fluorouracil tautomers by decorations of fullerene-like SiCs: DFT studies. *Physics Letters A* **2016,** *380*, 2160, https://doi.org/10.1016/j.physleta.2016.04.037.